PERFORMANCE OF PRESSURE EQUALIZED RAINSCREEN FACADES: A FIELD STUDY

J. D. Ginger and B. B. Yeatts
Wind Engineering Research Center, Texas Tech University, Lubbock Texas 79409, USA.

INTRODUCTION

The Pressure Equalized Rainscreen (PER) facade system has been acknowledged in the Building Industry as one of the most efficient methods of preventing rain penetration, caused by pressure differentials across openings in the building envelope. The PER facade system consists of three main components, i.) the rainscreen, consisting of vent holes on the building exterior ii.) the nominally air-tight air barrier, on the building interior and iii.) the pressure equalizing cavity vented to the building exterior. The sealant on the air barrier of the PER facade system is less susceptible to deterioration and failure compared to that on externally sealed facades. Ganguli and Dalgliesh (1988) measured smaller net pressures across the rainscreen compared to the net pressures across the composite wall, due to the "equalization" of cavity pressure with the external pressure. Therefore the building exterior may be designed with expensive lightweight materials at reduced cost.

EXPERIMENTAL SET UP

Tests were carried out on a 0.9 × 0.9 m × 80 mm deep PER facade element attached to the existing window opening, on the 9.1 × 13.7 × 4.0 m Texas Tech, Wind Engineering Research Field Laboratory (WERFL) test building shown in Fig 1. The approach terrain is open and the topography flat. A row of 12.7 mm diameter circular vent holes were drilled 80 mm from the bottom edge of the rainscreen. The facade was well sealed and the air-barrier was air-tight (i.e. $A_L \sim 0$). A range of venting areas A_V were studied by opening a selected number of vent holes at a time. External pressures, p_E were measured at mid height (elevation of 2.0 m) on the rainscreen, the cavity pressure, p_C was measured within the cavity at the mid height of the PER, and the building internal pressure p_I, was measured at different points within the building.

The pressure signals are low pass filtered at 8 Hz, and sampled at 30 Hz, for 15 mins for a single run. The mean, standard deviation, maximum and minimum pressure coefficients are defined as,

$$C_{\overline{p}} = \frac{\overline{p} - p_0}{(1/2)\rho \overline{U}^2}, \quad C_{\sigma p} = \frac{\sigma_p}{(1/2)\rho \overline{U}^2}, \quad C_{\hat{p}} = \frac{\hat{p} - p_0}{(1/2)\rho \overline{U}^2}, \quad C_{\check{p}} = \frac{\check{p} - p_0}{(1/2)\rho \overline{U}^2}, \qquad \text{where}$$

$\overline{p}, \sigma_p, \hat{p}, \check{p}$, are the mean, standard deviation, maximum and minimum pressure in a 15 min run, p_0, is the reference atmospheric pressure, ρ is the density of air and $\overline{U}$ is the mean wind speed at roof height (i.e. 4.0 m), over a 15 min run.

Results from averaging three runs, for wind orientations (α) of 180° ± 5° (i.e. wind flow normal to the PER causing maximum positive pressure difference across the wall and possible rain penetration) and 90° ± 5° (i.e. PER facade experiencing large suction pressures) are presented here.

THEORY

The theory of turbulent flow through an orifice is used to obtain the relationship between the mean external facade face pressure ($\overline{p}_E$), mean cavity pressure ($\overline{p}_C$) and mean internal building pressure ($\overline{p}_I$) on a PER facade with a total venting area to the exterior, A_V and air-barrier leakage area into the building A_L,

$$\frac{C_{\overline{p}_E} - C_{\overline{p}_C}}{C_{\overline{p}_C} - C_{\overline{p}_I}} = \frac{C_{\overline{p}_{RS}}}{C_{\overline{p}_{AB}}} = \left(\frac{A_L}{A_V}\right)^2 \qquad (1)$$

where, $C_{p_{RS}}$ and $C_{p_{AB}}$ are the net pressure coefficients across the rainscreen and air barrier.

The primary factors which influence the pressure within the cavity are the external and building interior pressure fields across the PER facade, and position and size of all openings connecting the cavity to these pressure fields. The response of the cavity pressure is also dependent on the cavity volume and stiffness of the PER facade skin. The natural frequency of a typical PER facade skin is usually well outside the frequencies of the approach wind flow and the fluctuating cavity pressures, and the PER facade skin may be considered to follow the loads in a quasi-static manner. The flexibility effects of the PER facade skin may be accounted for by increasing the nominal cavity volume V_C by a factor of the ratio of bulk modulus of air K_A to the bulk modulus of the facade, K_F. The cavity pressure dynamics can be modeled by using an effective cavity volume $V_{Ce} = V_C (1 + (K_A / K_F))$ similar to that described by Vickery (1986), for building internal pressure dynamics.

The motion of air within a cavity with a venting area A_V and leakage area $A_L \sim 0$, may be described by the Helmholtz, non-linear second order differential Equation 2, in terms of cavity pressure coefficient C_{pC} and external pressure coefficient, C_{pE} using an adiabatic process with a coefficient n, an opening discharge coefficient k, and effective length of slug of air moving in and out of the cavity, $l_e = \sqrt{\pi A_V}/4$.

$$\frac{\rho l_e V_{Ce}}{n p_0} \ddot{C}_{pC} + \frac{\rho^2 V_{Ce}^2 \overline{U}^2}{4k^2 n^2 A_V p_0^2} \dot{C}_{pC} \left| \dot{C}_{pC} \right| - A_V C_{pC} = A_V C_{pE} \qquad (2)$$

Holmes (1979) carried out wind tunnel tests on a building model over a range of single windward opening areas and showed that internal pressure resonance occurs close to the undamped resonant frequency, $f_0 = (1/2\pi)(nA_V p_0/\rho l_e V_{Ce})^{0.5}$.

RESULTS

The skin of the PER facade is constructed from flexible cladding material and $K_A/K_F = 12$. Therefore the effective interior volume V_{Ce} is $(0.9 \times 0.9 \times 0.08\ \text{m}) \times (1 + 12) = 0.84\ \text{m}^3$. The Helmholtz frequencies, f_0 are 8.6, 9.3 and 10.7 Hz, for 3, 5 and 7, 12.7 mm diameter vent holes (i.e. A_V = 380, 633 and 887 mm^2) studied here. The natural frequency of the PER facade skin was ~ 60 Hz and resonant effects are negligible.

The pressure coefficients on the external face of the facade, cavity and building interior for 3, 5 and 7, 12.7 mm diameter vent holes (i.e. A_V = 380, 633 and 887 mm^2), for wind orientations $\alpha \sim 180°$ and 90° are given in Table 1a. The corresponding net wall (i.e. external - building interior) net rainscreen (i.e. external - cavity) and net air-barrier (i.e. cavity - building interior) mean, standard deviation, maximum and minimum pressure coefficients are given in Table 1b.

Table 1a. Mean, standard deviation, maximum and minimum pressure coefficients on the external facade face, cavity and building interior.

α	A_V, mm^2	$C_{\bar{p}_E}$	$C_{\sigma_{pE}}$	$C_{\hat{p}_E}$	$C_{\check{p}_E}$	$C_{\bar{p}_C}$	$C_{\sigma_{pC}}$	$C_{\hat{p}_C}$	$C_{\check{p}_C}$	$C_{\bar{p}_I}$	$C_{\sigma_{pI}}$	$C_{\hat{p}_I}$	$C_{\check{p}_I}$
~180°	380	0.51	0.31	2.01	-0.16	0.50	0.31	1.98	-0.13	-0.23	0.10	0.16	-0.66
	633	0.56	0.28	1.89	-0.14	0.57	0.27	1.83	-0.01	-0.22	0.08	0.05	-0.62
	887	0.57	0.28	1.92	-0.33	0.56	0.27	1.93	-0.17	-0.23	0.08	0.07	-0.05
~90°	380	-0.44	0.29	0.42	-1.71	-0.44	0.28	0.36	-1.54	-0.21	0.10	0.24	-0.94

Table 1b. Net wall (external - internal), net rainscreen (external - cavity) and net air-barrier (cavity - internal) mean, standard deviation, maximum and minimum pressure coefficients.

α	A_V, mm^2	$C_{\bar{p}_W}$	$C_{\sigma_{pW}}$	$C_{\hat{p}_W}$	$C_{\check{p}_W}$	$C_{\bar{p}_{RS}}$	$C_{\sigma_{pRS}}$	$C_{\hat{p}_{RS}}$	$C_{\check{p}_{RS}}$	$C_{\bar{p}_{AB}}$	$C_{\sigma_{pAB}}$	$C_{\hat{p}_{AB}}$	$C_{\check{p}_{AB}}$
~180°	380	0.74	0.34	2.21	-0.01	0.01	0.05	0.30	-0.32	0.73	0.34	2.18	0.04
	633	0.78	0.31	2.32	0.13	-0.01	0.05	0.33	-0.41	0.79	0.30	2.37	0.04
	887	0.80	0.27	2.26	0.03	0.01	0.04	0.51	-0.37	0.79	0.27	2.23	0.15
~90°	380	-0.23	0.29	0.97	-1.51	0.00	0.07	0.68	-0.79	-0.23	0.28	0.93	-1.37

Table 1a, shows that the mean cavity pressures are equal to the mean external pressures on the facade face as expressed by Eqn 1, for $A_L = 0$. The mean internal building pressure is small and negative, ~ -0.20. Table 1b, shows that the net mean pressure across the wall is almost entirely taken by the air-barrier, and the net mean pressure across the rainscreen is small. For $\alpha \sim 180°$, the net peak positive pressures across the rainscreen are only ~ 20% of the net peak positive pressures across the wall. However a net rainscreen peak positive pressure ~ 30% of the net peak positive pressures across the wall is measured for $\alpha \sim 90°$. For $\alpha \sim$

90°, the net peak suction pressure across the rainscreen is ~55% of the net peak suction pressure across the wall. The net peak positive and peak suction pressures across the air-barrier are ~ 100% of the net pressures across the wall. Results show that pressure equalization was good over the venting areas studied. However increasing the venting area will provide better pressure equalization if air-barrier leakage is introduced.

Portions of typical pressure-time histories on the external facade face, cavity and building interior and the corresponding net pressures across the wall, rainscreen and air-barrier, for the rainscreen with 3 vent holes (i.e. A_V = 380 mm^2), for α ~ 180° and 90° are given in Figs 2 and 3 respectively. Figs 2 and 3 show that the pressure inside the cavity equalizes the external pressure, and the net pressure across the rainscreen is small.

The external facade face, cavity and building interior, non-dimensional pressure spectra $fS_p(f)/\left(\frac{1}{2}\rho\bar{U}^2\right)^2$ for the rainscreen with 3 vent holes, for α ~ 180° and 90° are shown in Figs 4a and 5a respectively. The net wall, net rainscreen and net air-barrier non-dimensional pressure spectra for the rainscreen with 3 vent holes, for α ~ 180° and 90° are shown in Figs 4b and 5b respectively. Figs. 4a and 5a show that the cavity pressure spectrum closely follows the external pressure spectrum over the lower frequency range (i.e. < 1.5 Hz). The building interior pressure fluctuations are smaller than the external pressure fluctuations. Figs 4b and 5b show that a major portion of external pressure fluctuations are transmitted into the cavity and are imposed on the air-barrier. The net pressure fluctuations across the rainscreen are small and contain the high frequency (i.e. > 1.5 Hz) content of the external pressure fluctuations.

CONCLUSIONS

The following conclusions are drawn from studying the performance of a PER facade system exposed to natural wind conditions, using a combination of theoretical analysis and full scale measurements.

For a PER facade with a nominally air tight air-barrier, the mean and fluctuating cavity pressures follow the external pressures. Therefore the net load on the rainscreen is small. The net peak positive and suction pressures across the rainscreen are less than 60% of the net peak positive and suction pressures across the building wall. The air-barrier experiences the entire net wall pressures. Spectral analysis indicates that the major portion of external pressure energy is transmitted into the cavity and experienced by the air-barrier. The net pressure fluctuations across the rainscreen are small and contain the higher frequencies.

REFERENCES

(1) Ganguli, U. and Dalgliesh, W. A. (1988), Wind Pressures on Open Rain Screen Walls: Place Air Canada, Jour. of Structural Engg., ASCE Vol. 114, No. 3, 642-656.

(2). Holmes, J. D. (1979), Mean and Fluctuating Internal Pressures Induced by wind, Proc. 5th Int. Conf. on Wind Engg., Colorado USA, Vol. 1, 435-450.

(3). Vickery, B. J. (1986), Gust factors for internal pressures in low rise buildings, Jour. of Wind Engineering and Industrial Aerodynamics, Vol. 23., 259-271.

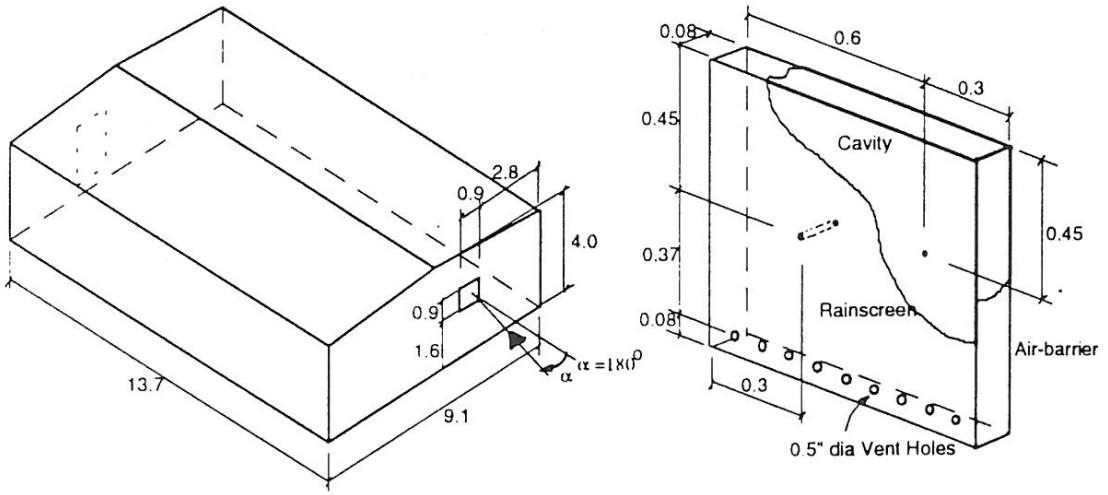

Figure 1. The full-scale WERFL test building and 0.9 × 0.9 × 0.08 m Pressure Equalized rainscreen Facade attached to window opening. (All dimensions in m)

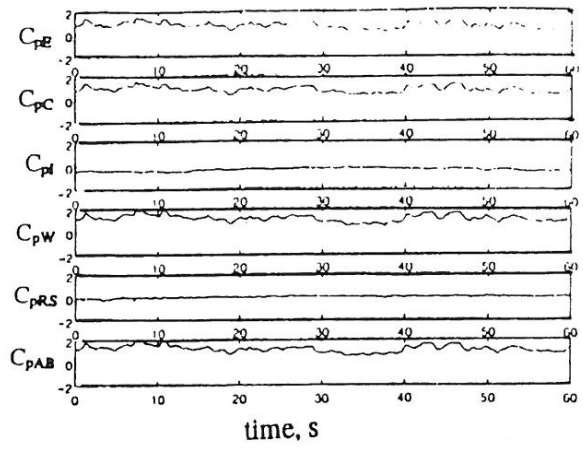

Fig 2. Typical Pressure vs. Time, $A_V = 380$ mm^2, $\alpha \sim 180°$

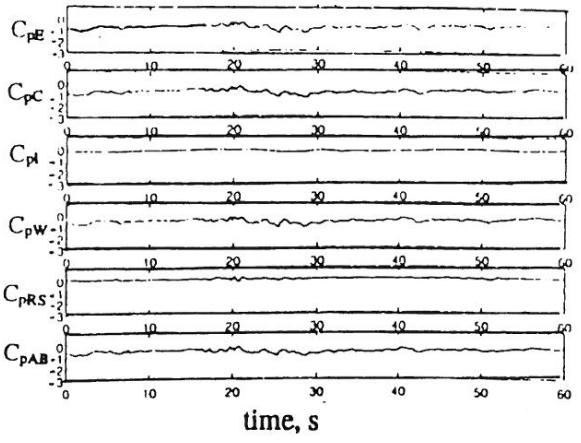

Fig 3. Typical Pressure vs. Time, $A_V = 380$ mm^2, $\alpha \sim 90°$

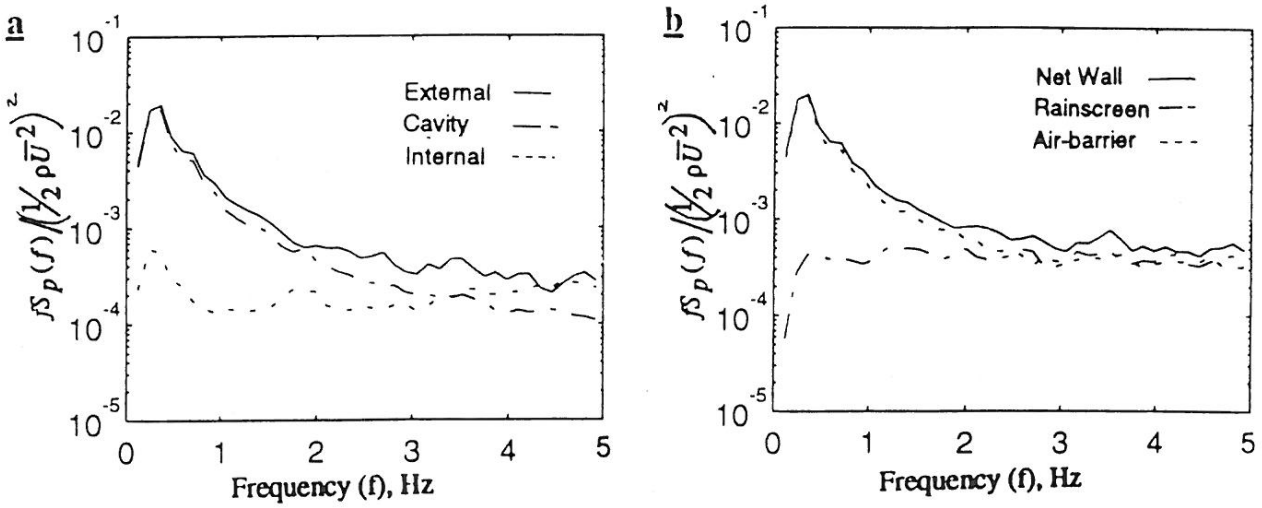

Fig 4. Non-Dimensional Pressure Spectra, $A_V = 380$ mm^2 $\alpha \sim 180°$

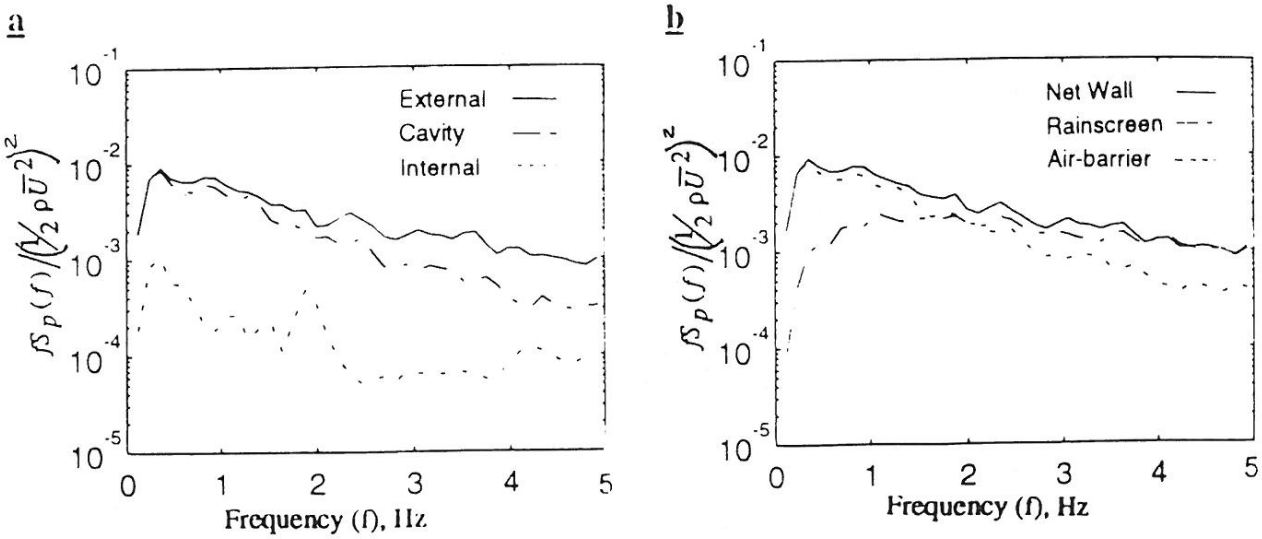

Fig 5. Non-Dimensional Pressure Spectra, $A_V = 380$ mm^2 $\alpha \sim 90°$